CHEMMEDCHEM

DOI: 10.1002/cmdc.200600244

Model Systems for Fluorescence and Singlet Oxygen Quenching by Metalloporphyrins

Jason R. McCarthy* and Ralph Weissleder[a]

Next-generation photodynamic therapy agents will minimize extraneous phototoxicity by being active only at the target site. To this end, we have developed a model system to systematically investigate the excited-state quenching ability of a number of metalloporphyrins. Central metal ions that prefer four-coordinate, square planar orientations (Ag^{II}, Cu^{II}, Ni^{II}, Pd^{II}, and Zn^{II}) were used. Porphyrin dimers based on 5-(4-aminophenyl)-10,15,20-triphenylporphyrin and comprising both a free base porphyrin and a metalloporphyrin covalently linked through a five-carbon alkyl chain were synthesized. The fluorescence and singlet oxygen quantum yields for the dimers were probed at 630 and 650 nm, respectively, resulting in the excitation of only the free base porphyrin and allowing a comparison of the quenching efficacy of each central metal ion. These results demonstrate that metalloporphyrins can serve as efficient quenchers, and may be useful in the design of novel light-activated therapeutic agents.

Introduction

Light-inducible, singlet oxygen producing drugs have been highly successful in treating a variety of human diseases. In particular, porphyrinic pigments have enjoyed widespread use as photodynamic therapy (PDT) agents in the treatment of cancers, age-related macular degeneration,[1–3] and most recently, cardiovascular disease.[4,5] Unfortunately, the therapeutic window of many agents is small, and the associated toxicity can be significant.[6] Over time, a number of modifications have been made to the porphyrins to increase their singlet oxygen quantum yields, make them more water soluble, improve their pharmacokinetics, and target them to tissues of interest. The latter approach has been a major focus, and photosensitizers have been targeted to tumors via peptides,[7] monoclonal antibodies,[8–10] and nanoparticulate delivery vehicles.[11,12] An alternative and novel strategy has been to synthesize enzyme-activatable PDT agents, that is, substrates for enzymes that are upregulated in certain diseases. For example, we recently described a cysteine protease activatable agent that uses multiple copies of chlorin e6 conjugated to a poly-L-lysine-co-monomethoxy-polyethylene glycol backbone, which is quenched by aggregation of the photosensitizer, and activated by cathepsins.[13]

Similar to activatable fluorescent probes, activatable PDT agents have been based largely on energy transfer between the photosensitizer and a quencher molecule,[14,15] or energy transfer between photosensitizers.[13] Thus far, minimal research has been undertaken to investigate the efficacy of transition-metal complexes in the quenching of singlet oxygen generation. It is well known that transition metals have the potential to accept electrons from excited-state molecules through electron- or energy-transfer processes, especially paramagnetic metal ions.[16–21] Therefore, we hypothesized that metalloporphyrins, metal-coordinating analogues of porphyrin-based photosensitizers, can act as efficient excited-state quenchers. We have thus systematically explored a number of analogues and tested their efficiency in the hybrid system depicted in Figure 1. To this end, a number of porphyrin dimers containing both a free base porphyrin and a metalloporphyrin were synthesized, and the quenching efficiency of each system was investigated. To limit the number of compounds, we chose metal ions such as Ag^{II}, Cu^{II}, Ni^{II}, Pd^{II}, and Zn^{II} that favor square planar, four-coordinate orientations in porphyrinic systems.

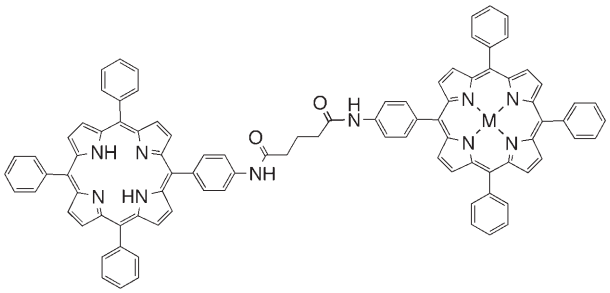

Figure 1. Structure of porphyrin–metalloporphyrin dimers **5M** for which M = Ag^{II}, Cu^{II}, Ni^{II}, Pd^{II}, Zn^{II}.

Results and Discussion

Synthesis and photophysical characterization of porphyrin–metalloporphyrin dimers

Ideally, a model system that results in amide bond formation would be preferred, as it allows control of dimer formation through commonly used coupling reagents. Hence, 5-(4-ami-

[a] *Dr. J. R. McCarthy, Prof. Dr. R. Weissleder*
Center for Molecular Imaging Research
Massachusetts General Hospital and Harvard Medical School
149 13th St., Rm 5406, Charlestown, MA 02129 (USA)
Fax: (+1) 617-726-5708
E-mail: jason_mccarthy@hms.harvard.edu

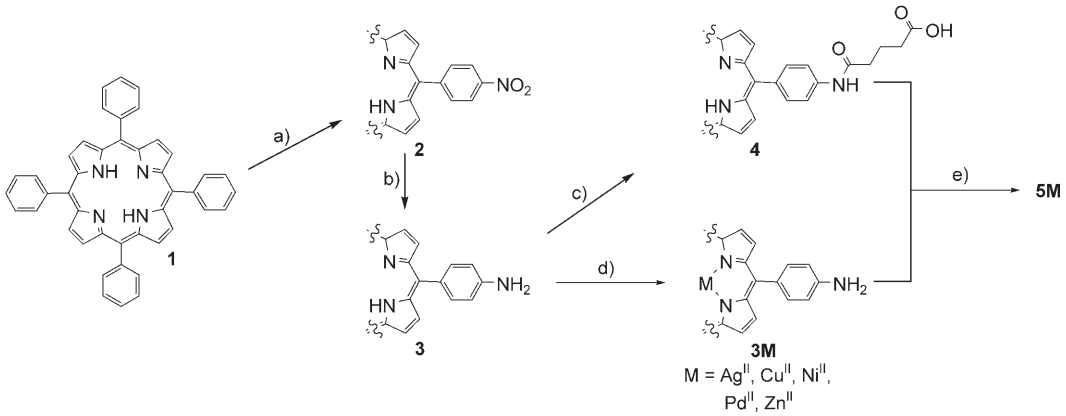

Scheme 1. Reaction conditions: a) $NaNO_2$, TFA, 5 min; b) $SnCl_2 \cdot 2H_2O$, HCl (concd); c) glutaric anhydride, DMF; d) microwave-assisted metallation for Ag^{II}, Cu^{II}, Ni^{II}, Zn^{II}; for Pd^{II}: $Pd(OTf)_2$, 1,2-dichloroethane/MeOH (3:1), 45 °C; e) DCC, CH_2Cl_2/pyridine (95:5). DCC = dicyclohexylcarbodiimide, DMF = *N*,*N*-dimethylformamide, TFA = trifluoroacetic acid.

nophenyl)-10,15,20-triphenylporphyrin **3** was chosen as our starting material, as it is easily synthesized from the corresponding 5,10,15,20-tetraphenylporphyrin (TPP, **1**) by nitration with $NaNO_2$ followed by reduction with $SnCl_2 \cdot 2H_2O$, as reported previously (Scheme 1).[22] Aminophenylporphyrin **3** can be further functionalized with a five-carbon linker terminating in an acid moiety by reaction with glutaric anhydride to give compound **4**.[23] The corresponding aminophenyl metalloporphyrins (**3Ag**, **3Cu**, **3Ni**, and **3Zn**) are formed by microwave-assisted reaction of **3** with the appropriate metal acetate in $CHCl_3$/pyridine, whereas **3Pd** is synthesized by heating a solution of **3** in 1,2-dichloroethane/methanol with palladium(II) trifluoroacetate.

The side band region of the UV/Vis absorption spectra of porphyrin **3** and its corresponding metallo derivatives are shown in Figure 2. Upon metallation, the four absorption maxima for the free base porphyrin condense to give two peaks, with the expected hypsochromic shift of the longest wavelength absorption. It should also be noted that there is no overlap between the absorption of the furthest red side band of **3** and any of the side bands of the metalloporphyrins. Upon dimerization, this allows excitation of the free base porphyrin at 650 nm without absorption by the metalloporphyrin, which enables direct comparison of the quenching efficiency of each metal.

The porphyrin dimers were synthesized by reaction of the carboxylic acid functionalized porphyrin **4** with the corresponding metallo-aminophenylporphyrin **3M** in the presence of dicyclohexylcarbodiimide (DCC) in a solution of CH_2Cl_2/pyridine. The components of the dimers are linked by a short alkyl chain, which ensures that the only electronic interactions are through space (for example, the porphyrinic π systems are not directly conjugated to one another). This eliminates electron-transfer processes that have been observed in other conjugated dimer systems.[24,25]

The UV/Vis absorption spectra of the dimers **5** are shown in Figure 3. As expected, the absorption of the free base porphyrin at 650 nm is spectrally distinct from the absorption of the

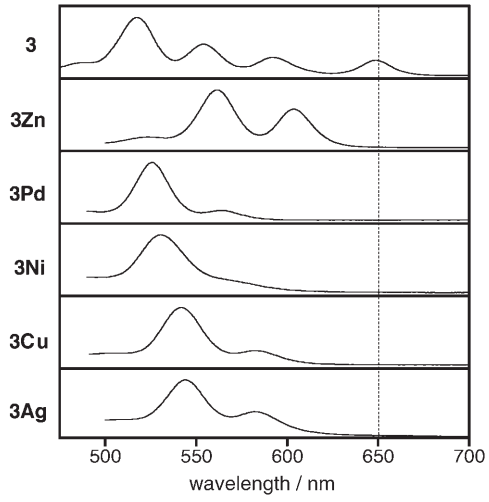

Figure 2. The side band region of the UV/Vis absorption spectra of porphyrin **3** and its corresponding metalloporphyrin derivatives in DMF. The dotted line represents the excitation wavelength for singlet oxygen generation.

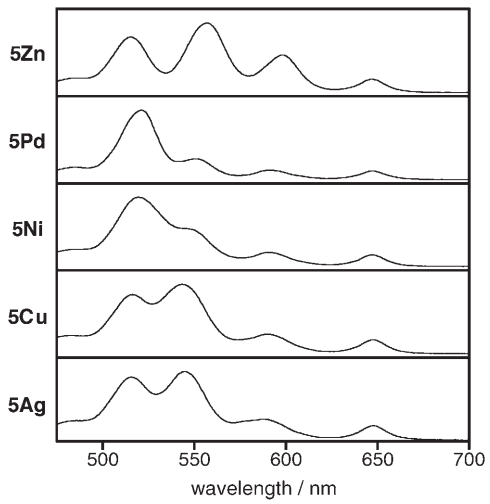

Figure 3. UV/Vis absorption spectra of dimers **5M**.

metalloporphyrins **3M**. We were thus able to calculate the fluorescence and singlet oxygen quantum yields for each dimer by using TPP as the standard (Table 1). The results of the excited-state quenching studies are detailed below. Control experiments were performed for each dimer system on solutions containing equimolar quantities of the porphyrin and metalloporphyrin monomers, with no observed quenching efficacy.

Table 1. Fluorescence and singlet oxygen quantum yields of the dimers.

	Fluorescence		Singlet Oxygen	
	ϕ_{Fl}[a]	Fold Decrease	ϕ_{Δ}[b]	Fold Decrease
TPP	0.15	--	0.64	--
5Ag	0.02	7.2	0.05	12.3
5Cu	0.10	1.6	0.41	1.6
5Ni	0.08	1.9	0.21	3.1
5Pd	0.21	0.7	0.52	1.2
5Zn	0.18	0.9	0.62	1.0

[a] In DMF, 630 nm excitation. [b] In DMF, 650 nm excitation.

Cu^{II} and Ni^{II} porphyrins as excited-state quenchers

Copper and nickel ions are present ubiquitously throughout the photophysical literature as excited-state quenchers.[26,27] With partially filled d orbitals, these metal ions are capable of fluorescence quenching by electron or energy transfer. Furthermore, Cu^{II}, with its d^9 valence electron configuration, is paramagnetic, which has been shown to increase the quenching efficiency of the metal ion.[20] As expected, both Cu^{II} and Ni^{II} demonstrate the ability to quench in our model system (Table 1). What is interesting is that Cu^{II} is not a more efficient excited-state quencher than Ni^{II}. In fact, Ni^{II} is 20% more efficient at quenching the fluorescence, and 200% more efficient at quenching the singlet oxygen generation of the free base porphyrin in dimer **5Ni** than Cu^{II} in **5Cu**. This is counter to previous examples,[28] and cannot be fully explained at this time.

Zn^{II} porphyrins as excited-state quenchers

Spectroscopically silent zinc is often the focus of fluorescence-based probes. Owing to its full d orbital, Zn^{II} is colorless and lacks d–d transitions.[29] It is, therefore, necessary to design molecular sensors that are activated upon zinc binding. These sensors are usually based on chelation-enhanced fluorescence in which the sensor is nonfluorescent until it binds the ion of interest.[29–31] If Zn^{II} acted as an excited-state quencher, this type of sensor would not be feasible. Moreover, Zn^{II} porphyrins are themselves fluorescent, further illustrating the excited-state behavior of this metal ion.[32] In the porphyrin–metalloporphyrin dimer system **5Zn** there is no observed excited-state quenching by the Zn^{II} metalloporphyrin (Table 1). This result is completely expected based on previous examples.

Ag^{II} porphyrins as excited-state quenchers

Silver ions are not often investigated for their ability to quench the excited states of chromophores. Even less common is the use of Ag^{II} as a quencher moiety, because a limited number of Ag^{II} compounds are known.[33] Ag^{I} has displayed the ability to quench fluorescence in a number of systems.[18,21,34] Being isoelectronic to diamagnetic Hg^{II}, which has well-documented chelation-enhanced quenching due to the heavy-atom effect, it is no surprise that Ag^{I} also acts as a quencher.[35] Ag^{II}, on the other hand, has a d^9 valence electron configuration and is paramagnetic, similar to Cu^{II}, while retaining the large size of its Ag^{I} counterpart. This combination of factors allowed us to hypothesize that Ag^{II} would serve as the best excited-state quencher. This assumption was entirely correct, as is illustrated by the 7.2-fold decrease in fluorescence quantum yield, as well as the 12.3-fold decrease in singlet oxygen quantum yield for system **5Ag** (Table 1).

Pd^{II} porphyrins as excited-state quenchers

Similar to Ag^{II}, there have been very few studies of the effect of the Pd^{II} metal ion on the excited-state quenching of chromophores. In one account the authors claim that Pd^{II} serves as a weak quencher of the fluorescence of pyridobenzimidazole nucleosides.[36] In this same study the authors also mention that Ni^{II} and Cu^{II} serve as strong quenchers. This is interesting, in that Ni^{II} and Pd^{II} share the same d^8 valence electron configuration, while the latter is larger and thus is expected to be the better quencher. This is not observed in our porphyrin–metalloporphyrin dimer system. As stated previously, the presence of Ni^{II} in **5Ni** results in a 1.9-fold decrease in fluorescence emission and a 3.1-fold decrease in singlet oxygen production of the free base porphyrin. In **5Pd** there is actually an increase in fluorescence emission (1.4-fold), while the singlet oxygen production remains unchanged (Table 1). This lack of quenching efficacy may be due to the fact that Pd^{II} porphyrins, similar to Zn^{II} porphyrins, are also known to be singlet oxygen generators.[37] In this study the three metal ions that are not singlet oxygen generators or luminophores (Ag^{II}, Cu^{II}, and Ni^{II}) exhibit the ability to quench the excited states of the free base porphyrin, whereas those which can luminesce or are known for their energy-transfer abilities do not.

Biological considerations

For the porphyrin–metalloporphyrin dimer systems to be viable in vivo, they must be first conjugated to a cleavable backbone, similar to previously described activatable fluorescence imaging agents.[38] In these systems the photosensitizer and quencher are separated by a short amino acid sequence that is recognized by a specific enzyme, such as a matrix metalloproteinase or cathepsin, which are often upregulated in cancer and other sites of inflammation. Upon cleavage of the peptide, the porphyrin and metalloporphyrin are no longer held in close proximity, and thus, will no longer be quenched. These peptide-based systems also allow further conjugation of

the activatable unit to a targeting moiety or a nanoparticulate vehicle for increased in vivo delivery.

One of the main considerations of the use of metalloporphyrins is the potential toxicity associated with the degradation of the porphyrinic macrocycle or dissociation of the central metal ion from the porphyrin core. Of those metal ions that showed quenching efficacy in our model system, Ni^{II} and Cu^{II} are bound strongly by the porphyrinic macrocycle and are not likely to dissociate from the porphyrin core, except under harsh conditions (stability constant, $\log\beta \approx 40\,M^{-1}$).[39,40] Whereas Ag^{II} is not as strongly bound as Cu^{II} or Ni^{II}, demetallation under physiological conditions is unlikely, as strongly acidic conditions are required to effect demetallation.[40] Although copper is considered an essential mineral (recommended intake of 2 mg day^{-1}), excess copper (>10 mg day^{-1}) is associated with toxicity.[41] Nickel, on the other hand, is considered intrinsically toxic, even at low levels.[42] Interestingly, the metal ion that exhibited the highest quenching efficiency, silver, is nontoxic and is not known to cause cancer or any other chronic adverse effects. In fact, silver is well known for its antimicrobial activity and is used in burn wound care and biomaterials.[43] Thus, the use of Ag^{II}, Cu^{II}, and Ni^{II} metalloporphyrins should pose little or no threat of toxicity in vivo.

Conclusions

We have thus demonstrated that metalloporphyrins, especially those containing Ag^{II}, can act as efficient quenchers of both fluorescence emission and singlet oxygen generation. The choice of TPP as the starting material is also beneficial, as it permits modulation of the polarity of the chromophore through substitution of the aryl groups, enabling the fine-tuning of the quenching molecule. The above results could have potentially wide-ranging implications in the design of next-generation PDT agents and in decreasing extraneous phototoxicity. First, the quenchers are highly efficient and can prevent phototoxicity in nontarget tissues such as the skin, one of the key problems associated with current drugs.[6] Second, protease-activatable constructs would be sufficiently small enough to be further targetable by a variety of means. For example, conjugation of the quenched system to nanoparticle surfaces[11] or graft copolymers[38] could be used to preferentially deliver these compounds to angiogenic regions in tumors through the enhanced permeability and retention (EPR) effect. Finally, as the chemistries used for the synthesis of the dimers is identical to those used in peptide conjugation, this study is expected to be immediately applicable to the design of more efficient activatable photodynamic therapy agents. Thus, we believe that the approaches described herein will be highly useful in the design of the next generation of imaging and therapeutic PDT constructs.

Experimental Section

General: All solvents and reagents used were reagent grade or better and were used as received. The analytical TLC plates were obtained from Whatman (aluminum backed, 250 μm, with UV indicator); preparative TLC plates (500 μm silica gel on glass) and the flash-column silica gel (standard grade, 60 Å, 32–63 mm) used were provided by Sorbent Technologies, Atlanta, GA (USA). ^1H and ^{13}C NMR spectra were recorded on a Bruker DRX-400 or Bruker Avance 500 and were referenced to residual solvent peaks. All NMR analyses were performed at room temperature in the solvents indicated. UV/Vis spectra were recorded on a Cary 50 spectrophotometer, and fluorescence emission spectra on a Horiba Jobin Yvon Fluorolog-3 spectrofluorometer (Edison, NJ, USA) retrofit with a water-cooled R 928 photomultiplier tube. ESI mass spectra were recorded on a Waters Micromass ZQ mass spectrometer in the solvents indicated. High-resolution ESI mass spectra were provided by the Department of Chemistry Instrumentation Facility, Massachusetts Institute of Technology. Microwave-assisted reactions were performed in a CEM Discover. The purity of all compounds was determined in the course of all NMR analyses.

Fluorescence quantum yield: Quantum yield measurements, performed by following published procedures,[44] were collected for samples with absorbance values between 0.01 and 0.10 OD in DMF at 630 nm using 5,10,15,20-tetraphenylporphyrin in argon-purged benzene as a standard ($\phi_{FI} = 0.11$). Briefly, a small amount of stock porphyrin or dimer solution in DMF was added to 2 mL DMF. The OD of the resulting solution was determined, at which point the fluorescence spectrum was acquired, exciting at 630 nm. Using the integrated area under the curve from 635 to 800 nm, the fluorescence quantum yields were determined from the following equation:

$$Q_x = Q_r\left(\frac{A_r}{A_x}\right)\left(\frac{\eta_x^2}{\eta_r^2}\right)\left(\frac{D_x}{D_r}\right)$$

for which Q is the quantum yield of the solution, A is the optical density of the solution, η is the refractive index of the solution, D is the integrated area under the curve of the spectrum, and x and r are the unknown and reference solutions, respectively. All quantum yield determinations were performed in triplicate. The linearity of the OD versus the fluorescence quantum yield was also ascertained to ensure negligible contribution due to reabsorption effects.

Singlet oxygen quantum yields: Singlet oxygen quantum yields were calculated as described previously and performed in triplicate.[7,12] All solutions were in DMF with 0.1 OD at 650 nm.

Synthesis and characterization of porphyrins and porphyrin dimers: 5,10,15,20-tetraphenylporphyrin was prepared according to the procedure described by Adler et al.[45] 5-(4-aminophenyl)-10,15,20-triphenylporphyrin **3** and its acid-functionalized analogue **4** were synthesized as described previously.[23]

*[5-(4-aminophenyl)-10,15,20-triphenylporphyrinato]silver(II) (**3Ag**):* Ag(OAc) (37 mg, 3 equiv) was added to 47 mg **3** (7.5×10^{-2} mmol) in 3 mL $CHCl_3$/pyridine (95:5) in an 8-mL microwave reaction vessel. The reaction was carried out by microwave irradiation with the following settings: $T = 100\,^{\circ}C$, $t = 5$ min, P_{max} = off. Upon completion, the solution was evaporated to dryness under reduced pressure, dissolved in CH_2Cl_2, purified by flash chromatography (CH_2Cl_2, silica gel), and evaporated to dryness to yield **3Ag** as a purple powder (37 mg, 67% yield). UV/Vis (CH_2Cl_2) λ_{max} ($\log\varepsilon$): 421 (5.41), 544 (4.72), 582 (3.91) nm; +ESIMS (30 V, CH_3CN/0.1% TFA) $m/z = 734.1$ [M^+]; HRMS (ESI of [MH^+], CH_3CN): m/z calcd for $C_{44}H_{29}AgN_5$: 735.1552, found: 737.1572.

*[5-(4-aminophenyl)-10,15,20-triphenylporphyrinato]copper(II) (**3Cu**):* $Cu(OAc)_2{\cdot}H_2O$ (27 mg, 2 equiv) was added to 42 mg **3** (6.8×

10^{-2} mmol) in 3 mL $CHCl_3$/pyridine (95:5) in an 8-mL microwave reaction vessel. The reaction was carried out by microwave irradiation with the following settings: $T=150\,^{\circ}C$, $t=5$ min, $P_{max}=$off. Upon completion, the solution was evaporated to dryness under reduced pressure, dissolved in CH_2Cl_2, purified by flash chromatography (CH_2Cl_2, silica gel), and evaporated to dryness to yield **3Cu** as an orange–purple powder (20 mg, 43% yield). This material was identical to that described previously.[46] UV/Vis (CH_2Cl_2) λ_{max} ($\log\varepsilon$): 417 (5.42), 542 (4.29), 582 (sh) nm; +ESIMS (30 V, CH_3CN/0.1% TFA) $m/z=691.3$ [MH^+]; HRMS (ESI of [MH^+], CH_3CN): m/z calcd for $C_{44}H_{29}CuN_5$: 691.1797, found: 691.1777.

[5-(4-aminophenyl)-10,15,20-triphenylporphyrinato]nickel(II) (***3Ni***): Ni$(OAc)_2\cdot 4H_2O$ (38 mg 3 equiv) was added to 47 mg **3** (7.6×10^{-2} mmol) in 3 mL $CHCl_3$/pyridine (95:5) in an 8-mL microwave reaction vessel. The reaction carried out by microwave irradiation with the following settings: $T=150\,^{\circ}C$, $t=5$ min, $P_{max}=$off. Upon completion, the solution was evaporated to dryness under reduced pressure, dissolved in CH_2Cl_2, purified by flash chromatography (CH_2Cl_2, silica gel), and evaporated to dryness to yield **3Ni** as an orange–purple powder (45 mg, 80% yield). This material was identical to that described previously.[46] UV/Vis (CH_2Cl_2) λ_{max} ($\log\varepsilon$): 418 (5.27), 530 (4.29), 568 (sh) nm; +ESIMS (30 V, CH_3CN) $m/z=686.5$ [MH^+]; HRMS (ESI of [MH^+], CH_3CN): m/z calcd for $C_{44}H_{29}NiN_5$: 686.1855, found: 686.1830.

[5-(4-aminophenyl)-10,15,20-triphenylporphyrinato]palladium(II) (***3Pd***): $Pd(OTf)_2$ (53 mg, 2 equiv) was added to 51 mg **3** (8.1×10^{-2} mmol) in 3 mL 1,2-dichloroethane/MeOH (8:2). The reaction was heated for 1 h at 45 °C. Upon completion, the solution was evaporated to dryness under reduced pressure, dissolved in CH_2Cl_2, purified by flash chromatography (CH_2Cl_2, silica gel), and evaporated to dryness to yield **3Pd** as an orange–purple powder (49 mg, 83% yield). UV/Vis (CH_2Cl_2) λ_{max} ($\log\varepsilon$): 418 (5.31), 526 (4.40), 564 (sh) nm; ^{1}H NMR (400 MHz, [D_5]pyridine): $\delta=4.98$ (br s, 2H), 6.08 (br s, 2H), 7.38 (br s, 2H), 7.63 (br s, 12H), 8.18 (br m, 10H), 9.05 (br s, 8H), 9.32 ppm (br s, 2H); ^{13}C NMR (100 MHz, [D_5]pyridine): $\delta=$ 114.0, 122.5, 122.8, 124.7, 127.8, 128.7, 130.4, 131.8, 131.9, 132.1, 135.0, 136.5, 142.4, 142.5, 142.6, 143.4, 149.9 ppm; +ESIMS (30 V, CH_3CN/0.1% TFA) $m/z=734.4$ [M^+]; HRMS (ESI of [MH^+], CH_3CN): m/z calcd for $C_{44}H_{29}PdN_5$: 734.1482, found: 734.1558.

[5-(4-aminophenyl)-10,15,20-triphenylporphyrinato]zinc(II) (***3Zn***): Zn$(OAc)_2\cdot 2H_2O$ (35 mg, 2 equiv) was added to 50 mg **3** (8.0×10^{-2} mmol) in 3 mL $CHCl_3$/pyridine (95:5) in an 8-mL microwave reaction vessel. The reaction was carried out by microwave irradiation with the following settings: $T=80\,^{\circ}C$, $t=5$ min, $P_{max}=$off. Upon completion, the solution was evaporated to dryness under reduced pressure, dissolved in CH_2Cl_2, purified by flash chromatography (CH_2Cl_2, silica gel), and evaporated to dryness to yield **3Zn** as a purple powder (46 mg, 83% yield). This material was identical to that described previously.[46] UV/Vis (CH_2Cl_2) λ_{max} ($\log\varepsilon$): 428 (5.62), 562 (4.27), 604 (4.10) nm; +ESIMS (30 V, CH_3CN/0.1% TFA) $m/z=$ 691.5 [M^+]; HRMS (ESI of [M^+], CH_3CN): m/z calcd for $C_{44}H_{29}ZnN_5$: 692.1793, found: 692.1776.

General procedure for the synthesis of porphyrin–metalloporphyrin dimers: Dicyclohexylcarbodiimide (2 equiv) was added to a stirring solution of **3M** and **4** (1:2 molar ratio, $\sim 1.5\times 10^{-2}$ mmol scale) in 3 mL $CHCl_3$/pyridine (95:5). The reaction was stirred for 4 h, at which time it was filtered and then evaporated to dryness under reduced pressure. The crude solid was redissolved in CH_2Cl_2/MeOH (98.5:1.5) and purified by flash chromatography (silica gel, CH_2Cl_2/MeOH (98.5:1.5)). All fractions containing the pure product were combined and evaporated to dryness. Dimers **5M** were dissolved in a minimal amount of CH_2Cl_2, precipitated by the addition of hexanes, and filtered to give the product in 75% yield.

Dimer ***5Ag***: UV/Vis (CH_2Cl_2) λ_{max} ($\log\varepsilon$): 423 (5.77), 515 (4.34), 545 (4.38), 588 (sh), 647 (3.69) nm; +ESIMS (30 V, CH_3CN/0.1% TFA) $m/z=1460.9$ [MH^+], 731.9 [M^{2+}]; HRMS (ESI of [MH^+], CH_3CN): m/z calcd for $C_{93}H_{65}AgN_{10}O_2$: 1460.4343, found: 1462.4346.

Dimer ***5Cu***: UV/Vis (CH_2Cl_2) λ_{max} ($\log\varepsilon$): 419 (5.91), 516 (4.42), 544 (4.49), 590 (3.95), 647 (3.80) nm; +ESIMS (30 V, CH_3CN/0.1% TFA) $m/z=1416.8$ [MH^+], 710.1 [M^{2+}]; HRMS (ESI of [MH^+], CH_3CN): m/z calcd for $C_{93}H_{65}CuN_{10}O_2$: 1416.4588, found: 1417.4573.

Dimer ***5Ni***: UV/Vis (CH_2Cl_2) λ_{max} ($\log\varepsilon$): 419 (5.80), 518 (4.45), 550 (sh), 590 (3.77), 647 (3.70) nm; ^{1}H NMR (400 MHz, [D_5]pyridine): $\delta=$ −2.40 (br s, 2H), 2.70 (m, 2H), 3.07 (m, 4H), 7.59 (br s, 6H), 7.79 (br m, 16H), 8.35 (br m, 12H), 8.56 (br m, 4H), 9.00 (s, 4H), 9.03 (d, $J=4.8$, 2H), 9.15 (d, $J=4.8$, 2H), 11.4 ppm (s, 2H); ^{13}C NMR (100 MHz, pyridine d-5): δ = 117.8, 118.0, 119.5, 120.5, 120.6, 124.2, 127.3, 127.4, 128.4, 132.6, 132.7, 133.9, 134.0, 134.4, 134.8, 134.8, 135.3, 136.3, 140.3, 140.9, 142.1, 142.8, 142.8, 143.1, 173.2 ppm; +ESIMS (30 V, CH_3CN/0.1% TFA) $m/z=1411.8$ [MH^+], 706.7 [M^{2+}]; HRMS (ESI of [MH^+], CH_3CN): m/z calcd for $C_{93}H_{65}NiN_{10}O_2$: 1411.4645, found: 1412.4691.

Dimer ***5Pd***: UV/Vis (CH_2Cl_2) λ_{max} ($\log\varepsilon$): 419 (5.90), 521 (4.62), 550 (4.11), 590 (3.78), 647 (3.75) nm; ^{1}H NMR (400 MHz, [D_5]pyridine): $\delta=$ −2.42 (br s, 2H), 2.70 (m, 2H), 3.04 (m, 4H), 7.59 (br m, 10H), 7.78 (br m, 13H), 8.06 (m, 2H), 8.30 (br m, 12H), 8.52 (m, 4H), 8.99 (m, 9H), 9.13 (m, 4H), 11.28 ppm (br s, 2H); ^{13}C NMR (100 MHz, [D_5]pyridine): δ = 36.5, 118.2, 127.1, 127.1, 128.1, 128.2, 129.3, 131.4, 134.3, 141.8, 141.8, 142.1, 142.2, 172.1 ppm; +ESIMS (30 V, CH_3CN/0.1% TFA) $m/z=1460.0$ [MH^+], 730.7 [M^{2+}]; HRMS (ESI of [MH^+], CH_3CN): m/z calcd for $C_{93}H_{65}PdN_{10}O_2$: 1460.4351, found: 1459.4373.

Dimer ***5Zn***: UV/Vis (CH_2Cl_2) λ_{max} ($\log\varepsilon$): 426 (5.83), 516 (4.27), 556 (4.36), 597 (4.09), 647 (3.67) nm; ^{1}H NMR (400 MHz, [D_7]DMF): $\delta=$ −2.77 (s, 2H), 2.36 (p, $J=5.6$ Hz, 2H), 2.85 (m, 4H), 7.85 (br m, 18H), 8.30 (br m, 20H), 8.89 (s, 4H), 8.91 (d, $J=4.0$ Hz, 2H), 8.94 (br m, 6H), 9.01 (d, $J=3.6$ Hz, 2H), 9.06 (d, $J=3.2$ Hz, 2H), 10.5 (s, 1H), 10.6 ppm (s, 1H); ^{13}C NMR (100 MHz, [D_7]DMF): $\delta=$21.8, 36.6, 117.6, 117.9, 120.5, 120.6, 120.7, 120.8, 120.9, 121.0, 124.0, 126.9, 127.3, 127.8, 128.4, 131.4, 131.5, 131.5, 131.6, 131.7, 131.8, 131.9, 132.0, 132.1, 134.8, 135.2, 135.3, 136.5, 136.6, 138.1, 139.8, 140.3, 142.1, 142.2, 143.6, 148.6, 150.2, 150.3, 150.5, 171.9, 172.0 ppm; +ESIMS (30 V, CH_3CN/0.1% TFA) $m/z=1418.0$ [MH^+], 710.0 [M^{2+}]; HRMS (ESI of [MH^+], CH_3CN): m/z calcd for $C_{93}H_{65}ZnN_{10}O_2$: 1417.4583, found: 1419.4587.

Acknowledgements

We thank Dr. Ching H. Tung for his helpful discussions. This work was supported by NIH Grants UO1-HL080731-02 and U54-CA119349-01 to R.W.

Keywords: excited-state quenching · fluorescence · photodynamic therapy · porphyrin dimers · singlet oxygen

[1] D. E. Dolmans, D. Fukumura, R. K. Jain, *Nat. Rev. Cancer* **2003**, *3*, 380–387.

[2] R. K. Pandey, G. Zheng in *The Porphyrin Handbook, Vol. 6* (Eds.: K. M. Kadish, K. M. Smith, R. Guilard), Academic Press, San Diego, **2000**, pp. 157–230.

[3] E. D. Sternberg, D. Dolphin, C. Brückner, *Tetrahedron* **1998**, *54*, 4151 – 4202.
[4] S. G. Rockson, P. Kramer, M. Razavi, A. Szuba, S. Filardo, P. Fitzgerald, J. P. Cooke, S. Yousuf, A. R. DeVault, M. F. Renschler, D. C. Adelman, *Circulation* **2000**, *102*, 2322 – 2324.
[5] S. G. Rockson, D. P. Lorenz, W.-F. Cheong, K. W. Woodburn, *Circulation* **2000**, *102*, 591 – 596.
[6] M. B. Vrouenraets, G. W. Visser, G. B. Snow, G. A. van Dongen, *Anticancer Res.* **2003**, *23*, 505 – 522.
[7] Y. Choi, J. R. McCarthy, R. Weissleder, C.-H. Tung, *ChemMedChem* **2006**, *1*, 458 – 463.
[8] S. K. Bisland, D. Singh, J. Gariépy, *Bioconjugate Chem.* **1999**, *10*, 982 – 992.
[9] L. Chaloin, P. Bigey, C. Loup, M. Marin, N. Galeotti, M. Piechaczyk, F. Heitz, B. Meunier, *Bioconjugate Chem.* **2001**, *12*, 691 – 700.
[10] R. Hudson, R. W. Boyle, *J. Porphyrins Phthalocyanines* **2004**, *8*, 954 – 975.
[11] J. R. McCarthy, F. A. Jaffer, R. Weissleder, *Small* **2006**, *2*, 983 – 987.
[12] J. R. McCarthy, J. M. Perez, C. Brückner, R. Weissleder, *Nano Lett.* **2005**, *5*, 2552 – 2556.
[13] Y. Choi, R. Weissleder, C. H. Tung, *Cancer Res.* **2006**, *66*, 7225 – 7229.
[14] J. Chen, K. Stefflova, M. J. Niedre, B. C. Wilson, B. Chance, J. D. Glickson, G. Zheng, *J. Am. Chem. Soc.* **2004**, *126*, 11 450 – 11 451.
[15] K. Stefflova, J. Chen, D. Marotta, H. Li, G. Zheng, *J. Med. Chem.* **2006**, *49*, 3850.
[16] A. Harriman, *J. Chem. Soc. Faraday Trans. 2* **1981**, *77*, 1281 – 2191.
[17] D. Husain, T. Banfield, *Trans. Faraday Soc.* **1969**, *65*, 1985 – 1991.
[18] H. Masuhara, H. Shioyama, T. Saito, K. Hamada, S. Yasoshima, N. Mataga, *J. Phys. Chem.* **1984**, *88*, 5868 – 5873.
[19] W. M. Moore, G. S. Hammond, R. P. Foss, *J. Chem. Phys.* **1960**, *32*, 1594 – 1595.
[20] K. Rurack, *Spectrochim. Acta Part A* **2001**, *57*, 2161 – 2195.
[21] A. W. Varnes, R. B. Dodson, E. L. Wehry, *J. Am. Chem. Soc.* **1972**, *94*, 946 – 950.
[22] R. Luguya, L. Jaquinod, F. R. Fronczek, M. Graça H. Vicente, K. M. Smith, *Tetrahedron* **2004**, *60*, 2757 – 2763.
[23] M. Sibrian-Vazquez, T. J. Jensen, F. R. Fronczek, R. P. Hammer, M. G. Vicente, *Bioconjugate Chem.* **2005**, *16*, 852 – 863.
[24] A. B. Lysenko, P. Thamyongkit, I. Schmidt, J. R. Diers, D. F. Bocian, J. S. Lindsey, *J. Porphyrins Phthalocyanines* **2006**, *10*, 22 – 32.
[25] A. Muranaka, Y. Asano, A. Tsuda, A. Osuka, N. Kobayashi, *ChemPhysChem* **2006**, *7*, 1235 – 1240.
[26] M. H. Lim, D. Xu, S. J. Lippard, *Nat. Chem. Biol.* **2006**, *2*, 375 – 380.
[27] E. Rampazzo, E. Brasola, S. Marcuz, F. Mancin, P. Tecilla, U. Tonellato, *J. Mater. Chem.* **2005**, *15*, 2687 – 2696.
[28] R. L. Brookfield, H. Ellul, A. Harriman, *J. Chem. Soc. Faraday Trans. 2* **1985**, *81*, 1837 – 1848.
[29] N. C. Lim, H. C. Freake, C. Brückner, *Chem. Eur. J.* **2005**, *11*, 38 – 49.
[30] N. C. Lim, J. V. Schuster, M. C. Porto, M. A. Tanudra, L. Yao, H. C. Freake, C. Brückner, *Inorg. Chem.* **2005**, *44*, 2018 – 2030.
[31] N. C. Lim, L. Yao, H. C. Freake, C. Brückner, *Bioorg. Med. Chem. Lett.* **2003**, *13*, 2251 – 2254.
[32] G. D. Dorough, J. R. Miller, F. M. Huennekens, *J. Am. Chem. Soc.* **1951**, *73*, 4315 – 4320.
[33] J. R. McCarthy, S. H. Capetta, P. J. Melfi, C. Brückner, *Tetrahedron* **2003**, *59*, 9137 – 9146.
[34] M. Shamsipur, K. Alizadeh, M. Hosseini, C. Caltagirone, V. Lippolis, *Sens. Actuators B* **2006**, *113*, 892 – 899.
[35] E. U. Akkaya, M. E. Huston, A. W. Czarnik, *J. Am. Chem. Soc.* **1990**, *112*, 3590 – 3593.
[36] S. J. Kim, E. T. Kool, *J. Am. Chem. Soc.* **2006**, *128*, 6164 – 6171.
[37] A. Wiehe, H. Stollberg, S. Runge, A. Paul, M. O. Senge, B. Roder, *J. Porphyrins Phthalocyanines* **2001**, *5*, 853 – 860.
[38] R. Weissleder, C. H. Tung, U. Mahmood, A. Bogdanov, Jr., *Nat. Biotechnol.* **1999**, *17*, 375 – 378.
[39] H. R. Jimenez, M. Julve, J. Faus, *J. Chem. Soc. Dalton Trans.* **1991**, 1945 – 1949.
[40] J. W. Buchler in *Porphyrins and Metalloporphyrins*, 2nd ed. (Ed.: K. M. Smith), Elsevier Scientific Publishing Company, Amsterdam, **1975**, pp. 157 – 232.
[41] J. Bertinato, M. R. L'Abbé, *J. Nutr. Biochem.* **2004**, *15*, 316 – 322.
[42] T. P. Coogan, D. M. Latta, E. T. Snow, M. Costa, *Crit. Rev. Toxicol.* **1989**, *19*, 341 – 384.
[43] V. Alt, T. Bechert, P. Steinrucke, M. Wagener, P. Seidel, E. Dingeldein, E. Domann, R. Schnettler, *Biomaterials* **2004**, *25*, 4383 – 4391.
[44] J. N. Demas, G. A. Crosby, *J. Phys. Chem.* **1971**, *75*, 991 – 1024.
[45] A. D. Adler, F. R. Longo, J. D. Finarelli, J. Goldmacher, J. Assour, L. Korsakoff, *J. Org. Chem.* **1967**, *32*, 476 – 477.
[46] E. Barragán, B. Gordillo, G. Vargas, L. Velazco, *Appl. Organomet. Chem.* **2004**, *18*, 311 – 317.

Received: October 18, 2006
Revised: November 27, 2006
Published online on January 23, 2007

